Two-Body B Meson Decays to η and η': Observation of $B \to \eta' K$

B. H. Behrens,[1] W. T. Ford,[1] A. Gritsan,[1] H. Krieg,[1] J. Roy,[1] J. G. Smith,[1] M. Zhao,[1] J. P. Alexander,[2] R. Baker,[2] C. Bebek,[2] B. E. Berger,[2] K. Berkelman,[2] K. Bloom,[2] V. Boisvert,[2] D. G. Cassel,[2] D. S. Crowcroft,[2] M. Dickson,[2] S. von Dombrowski,[2] P. S. Drell,[2] K. M. Ecklund,[2] R. Ehrlich,[2] A. D. Foland,[2] P. Gaidarev,[2] L. Gibbons,[2] B. Gittelman,[2] S. W. Gray,[2] D. L. Hartill,[2] B. K. Heltsley,[2] P. I. Hopman,[2] J. Kandaswamy,[2] P. C. Kim,[2] D. L. Kreinick,[2] T. Lee,[2] Y. Liu,[2] N. B. Mistry,[2] C. R. Ng,[2] E. Nordberg,[2] M. Ogg,[2,*] J. R. Patterson,[2] D. Peterson,[2] D. Riley,[2] A. Soffer,[2] B. Valant-Spaight,[2] C. Ward,[2] M. Athanas,[3] P. Avery,[3] C. D. Jones,[3] M. Lohner,[3] S. Patton,[3] C. Prescott,[3] J. Yelton,[3] J. Zheng,[3] G. Brandenburg,[4] R. A. Briere,[4] A. Ershov,[4] Y. S. Gao,[4] D. Y.-J. Kim,[4] R. Wilson,[4] H. Yamamoto,[4] T. E. Browder,[5] Y. Li,[5] J. L. Rodriguez,[5] T. Bergfeld,[6] B. I. Eisenstein,[6] J. Ernst,[6] G. E. Gladding,[6] G. D. Gollin,[6] R. M. Hans,[6] E. Johnson,[6] I. Karliner,[6] M. A. Marsh,[6] M. Palmer,[6] M. Selen,[6] J. J. Thaler,[6] K. W. Edwards,[7] A. Bellerive,[8] R. Janicek,[8] D. B. MacFarlane,[8] P. M. Patel,[8] A. J. Sadoff,[9] R. Ammar,[10] P. Baringer,[10] A. Bean,[10] D. Besson,[10] D. Coppage,[10] C. Darling,[10] R. Davis,[10] S. Kotov,[10] I. Kravchenko,[10] N. Kwak,[10] L. Zhou,[10] S. Anderson,[11] Y. Kubota,[11] S. J. Lee,[11] J. J. O'Neill,[11] R. Poling,[11] T. Riehle,[11] A. Smith,[11] M. S. Alam,[12] S. B. Athar,[12] Z. Ling,[12] A. H. Mahmood,[12] S. Timm,[12] F. Wappler,[12] A. Anastassov,[13] J. E. Duboscq,[13] D. Fujino,[13,†] K. K. Gan,[13] T. Hart,[13] K. Honscheid,[13] H. Kagan,[13] R. Kass,[13] J. Lee,[13] M. B. Spencer,[13] M. Sung,[13] A. Undrus,[13,‡] A. Wolf,[13] M. M. Zoeller,[13] B. Nemati,[14] S. J. Richichi,[14] W. R. Ross,[14] H. Severini,[14] P. Skubic,[14] M. Bishai,[15] J. Fast,[15] J. W. Hinson,[15] N. Menon,[15] D. H. Miller,[15] E. I. Shibata,[15] I. P. J. Shipsey,[15] M. Yurko,[15] S. Glenn,[16] Y. Kwon,[16,§] S. Roberts,[16] E. H. Thorndike,[16] C. P. Jessop,[17] K. Lingel,[17] H. Marsiske,[17] M. L. Perl,[17] V. Savinov,[17] D. Ugolini,[17] R. Wang,[17] X. Zhou,[17] T. E. Coan,[18] V. Fadeyev,[18] I. Korolkov,[18] Y. Maravin,[18] I. Narsky,[18] V. Shelkov,[18] J. Staeck,[18] R. Stroynowski,[18] I. Volobouev,[18] J. Ye,[18] M. Artuso,[19] F. Azfar,[19] A. Efimov,[19] M. Goldberg,[19] D. He,[19] S. Kopp,[19] G. C. Moneti,[19] R. Mountain,[19] S. Schuh,[19] T. Skwarnicki,[19] S. Stone,[19] G. Viehhauser,[19] X. Xing,[19] J. Bartelt,[20] S. E. Csorna,[20] V. Jain,[20,‖] K. W. McLean,[20] S. Marka,[20] R. Godang,[21] K. Kinoshita,[21] I. C. Lai,[21] P. Pomianowski,[21] S. Schrenk,[21] G. Bonvicini,[22] D. Cinabro,[22] R. Greene,[22] L. P. Perera,[22] G. J. Zhou,[22] M. Chadha,[23] S. Chan,[23] G. Eigen,[23] J. S. Miller,[23] C. O'Grady,[23] M. Schmidtler,[23] J. Urheim,[23] A. J. Weinstein,[23] F. Würthwein,[23] D. W. Bliss,[24] G. Masek,[24] H. P. Paar,[24] S. Prell,[24] V. Sharma,[24] D. M. Asner,[25] J. Gronberg,[25] T. S. Hill,[25] D. J. Lange,[25] R. J. Morrison,[25] H. N. Nelson,[25] T. K. Nelson,[25] D. Roberts,[25] and A. Ryd[25]

(CLEO Collaboration)

[1]*University of Colorado, Boulder, Colorado 80309-0390*
[2]*Cornell University, Ithaca, New York 14853*
[3]*University of Florida, Gainesville, Florida 32611*
[4]*Harvard University, Cambridge, Massachusetts 02138*
[5]*University of Hawaii at Manoa, Honolulu, Hawaii 96822*
[6]*University of Illinois, Urbana-Champaign, Illinois 61801*
[7]*Carleton University, Ottawa, Ontario, Canada K1S 5B6*
and the Institute of Particle Physics, Canada
[8]*McGill University, Montréal, Québec, Canada H3A 2T8*
and the Institute of Particle Physics, Canada
[9]*Ithaca College, Ithaca, New York 14850*
[10]*University of Kansas, Lawrence, Kansas 66045*
[11]*University of Minnesota, Minneapolis, Minnesota 55455*
[12]*State University of New York at Albany, Albany, New York 12222*
[13]*Ohio State University, Columbus, Ohio 43210*
[14]*University of Oklahoma, Norman, Oklahoma 73019*
[15]*Purdue University, West Lafayette, Indiana 47907*
[16]*University of Rochester, Rochester, New York 14627*
[17]*Stanford Linear Accelerator Center, Stanford University, Stanford, California 94309*
[18]*Southern Methodist University, Dallas, Texas 75275*
[19]*Syracuse University, Syracuse, New York 13244*
[20]*Vanderbilt University, Nashville, Tennessee 37235*
[21]*Virginia Polytechnic Institute and State University, Blacksburg, Virginia 24061*
[22]*Wayne State University, Detroit, Michigan 48202*
[23]*California Institute of Technology, Pasadena, California 91125*
[24]*University of California, San Diego, La Jolla, California 92093*
[25]*University of California, Santa Barbara, California 93106*
(Received 5 January 1998)

 0031-9007/98/80(17)/3710(5)$15.00

In a sample of 6.6×10^6 produced B mesons we have observed decays $B \to \eta' K$, with branching fractions $\mathcal{B}(B^+ \to \eta' K^+) = (6.5^{+1.5}_{-1.4} \pm 0.9) \times 10^{-5}$ and $\mathcal{B}(B^0 \to \eta' K^0) = (4.7^{+2.7}_{-2.0} \pm 0.9) \times 10^{-5}$. We have searched with comparable sensitivity for 17 related decays to final states containing an η or η' meson accompanied by a single particle or low-lying resonance. Our upper limits for these constrain theoretical interpretations of the $B \to \eta' K$ signal. [S0031-9007(98)05921-3]

PACS numbers: 13.25.Hw, 14.40.Nd

The dominant decay modes of B mesons involve the $\overline{b} \to \overline{c}$ quark transition with coupling to a W^+ boson. For many of these modes the decay amplitude may be described by a tree diagram in which the light quark (spectator) is bound in both the initial B meson and final charmed hadron via soft gluon exchange. With recent improvements in experimental sensitivity, less favored modes are becoming accessible. These include $b \to u$ tree diagram transitions that are suppressed by the small Cabibbo-Kobayashi-Maskawa [1] matrix element V_{ub}, such as $B \to \pi \ell \nu$ [2]; effective flavor changing neutral current decays $b \to s$ described by loop diagrams, such as the "electromagnetic penguin" $B \to K^* \gamma$ [3]; and decays to charmless hadrons such as $B \to K\pi$ [4–6]. The hadronic decays may be classified according to contributions to the amplitude from several tree and penguin diagrams shown in Fig. 1 [7,8]. Some of these charmless hadronic decays offer prospects for the observation of CP violation, while others facilitate the quantitative understanding of the amplitudes that are essential to the interpretation of future CP measurements. For example, the decays $B \to \eta K$ and $B \to \eta' K$, with $B \to K\pi$, have been examined in this context [9,10].

In this paper we present results of experimental searches for B meson decays to two-body final states containing η and η' mesons. These $I = 0$ mesons are mixtures of flavor-SU(3) octet and singlet states, the latter being of particular interest because of its allowed formation through a pure (two or more) gluon intermediate state [Fig. 1(d)].

The data were accumulated at the Cornell Electron-positron Storage Ring. The integrated luminosity was $3.11\ \mathrm{fb}^{-1}$ for the reaction $e^+e^- \to \Upsilon(4S) \to B\overline{B}$ (center-of-mass energy $E_{\mathrm{cm}} = 10.58$ GeV). This luminosity corresponds to the production of 3.3×10^6 charged and an approximately equal number of neutral B mesons. In addition we recorded $1.61\ \mathrm{fb}^{-1}$ of data with E_{cm} below the threshold for $B\overline{B}$ production to measure continuum processes.

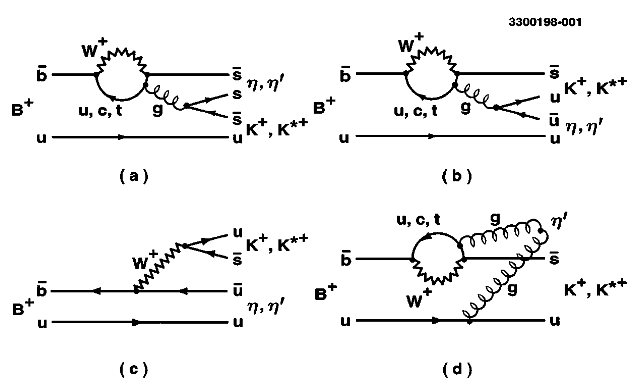

FIG. 1. Feynman diagrams describing the representative decays $B^+ \to \eta^{(\prime)} K^{(*)+}$: (a),(b) internal penguins; (c) external tree; (d) flavor-singlet penguin.

The CLEO II detector [11] emphasizes precision charged particle tracking, with specific ionization (dE/dx) measurement, and high resolution electromagnetic calorimetry based on CsI(Tl). From the raw data we reconstruct charged pions and kaons, photons (from π^0, η, and η' decays), and $\pi^+\pi^-$ pairs that intersect at a vertex displaced by at least 3 mm from the collision point ("vees," from $K_s^0 \to \pi^+\pi^-$). Candidate B decay tracks must meet specifications on the number of drift chamber measurements, goodness of fit, and consistency with an origin at the primary or particular secondary vertex. Candidate photons must be isolated calorimeter clusters with a photonlike spatial distribution and energy deposition exceeding 30 MeV. We exclude photon pairs from extremely asymmetric π^0 or η decays to reject soft photon backgrounds, requiring $|\cos\theta^*| < 0.97$, where θ^* is the meson center-of-mass decay angle relative to its flight direction. We reject charged tracks and photon pairs having momentum less than 100 MeV/c.

We fit photon pairs and vees kinematically to the appropriate combined mass hypothesis to obtain the meson momentum vectors. Resolutions on the reconstructed masses prior to the constraint are about 5–10 MeV/c^2 (momentum dependent) for $\pi^0 \to \gamma\gamma$, 12 MeV/c^2 for $\eta \to \gamma\gamma$, and 3 MeV/c^2 for $K_s^0 \to \pi^+\pi^-$. Information about expected signal distributions with the detector response comes from a detailed GEANT based simulation of the CLEO detector [12] that reproduces the resolutions and efficiencies of data in a variety of benchmark processes.

Since the B mesons are formed nearly at rest, while the B daughters we observe are relatively light, the latter have momenta close to half of the beam energy (2.6 GeV/c). For this reason the final states are well separated from those involving heavier daughters, i.e., the dominant $b \to c$ decays. The principal signatures for the selected decay modes are consistency of the resonance decay invariant masses with the known masses and widths of those resonances, and consistency of the total final state with the B meson mass and energy. Because the beam energy E_b is better known than the reconstructed B meson energy E_B, we substitute the former in the B mass calculation: $M \equiv \sqrt{E_b^2 - \mathbf{p}_B^2}$, with $\mathbf{p}_B$ the reconstructed B momentum. We also define the variable $\Delta E \equiv E_B - E_b$. The measurement resolution on M is about 2.6 MeV/c^2, and on ΔE it is 25–40 MeV, depending on the apportionment of the energy among charged tracks and photons for each mode.

For vector-pseudoscalar decays of the B and $\rho\gamma$ decays of the η' we gain further discrimination from the helicity variable $\mathcal{H}$ (cosine of the vector meson's rest frame two-body decay angle with respect to its flight direction), which reflects the spin alignment in the decay. For modes in which one daughter is a single charged track, or is a resonance pairing a charged track with a π^0, we achieve statistical discrimination between kaons and pions by dE/dx. With S_K and S_π defined as the deviations from nominal energy loss for the indicated particle hypotheses measured in standard deviations, the separation $S_K - S_\pi$ is about 1.7 at 2.6 GeV/c.

The main backgrounds arise from continuum quark production $e^+e^- \to q\overline{q}$. We discriminate against these jetlike events with several measures of the energy flow pattern. One is the angle θ_{BB} between the thrust axis (axis of maximum energy projection magnitude) of the candidate B and that of the rest of the event. For a fake B candidate selected from particles belonging to a $q\overline{q}$ event those particles tend to align with the rest of the event, whereas the true B decays have a thrust axis that is largely uncorrelated with the tracks and showers from the decay of the partner B. We reject events with $|\cos\theta_{BB}| > 0.9$. In addition we use a multivariate discriminant $\mathcal{F}$ incorporating the energy deposition in nine cones concentric with the event thrust axis, and the angles of the thrust axis and $\mathbf{p}_B$ with respect to the e^+e^- beam direction [5]. We have checked the backgrounds from the favored B decay modes by simulation and found their contributions to the modes in this study to be negligible.

To extract event yields we perform unbinned maximum likelihood fits to the data, including sidebands about the expected mass and energy peaks, of a superposition of expected signal and background distributions:

$$\mathcal{L}(N_S, N_B) = e^{-(N_S+N_B)} \times \prod_{i=1}^{N} [N_S \mathcal{P}_S(\vec{\beta}; \mathbf{x}_i) + N_B \mathcal{P}_B(\vec{\gamma}; \mathbf{x}_i)]. \quad (1)$$

Here $\mathcal{P}_S$ and $\mathcal{P}_B$ are the probability distribution functions (PDFs) for signal and continuum background, respectively. They are functions of observables $\mathbf{x}_i$ for event i, and of parameters $\vec{\beta}$ and $\vec{\gamma}$ (discussed below). The form of $\mathcal{L}$ reflects the underlying Poisson statistics obeyed by N_S and N_B, the (non-negative) numbers of signal and continuum background events, respectively, whose expectation values sum to the total number N of input events. Observables for each event include M, ΔE, $\mathcal{F}$, and (where applicable) resonance masses and $\mathcal{H}$. Where two modes involve a charged hadron (generically h^+) that is either π^+ or K^+ we fit both simultaneously, with $\mathcal{L}$ expanded so that the signal and background yields of both π^+ and K^+ are fit variables. In this case the PDFs also depend on the dE/dx observables S_π and S_K. The number of events N for these fits ranges from $\sim$30 to a few thousand.

TABLE I. Measurement results. Columns list the final states (with secondary decay modes as subscripts), event yield from the fit, reconstruction efficiency ϵ, total efficiency with secondary branching fractions $\mathcal{B}_s$, and the resulting B decay branching fraction $\mathcal{B}$.

Final state	Fit events	ϵ(%)	$\epsilon\mathcal{B}_s$(%)	$\mathcal{B}(10^{-5})$
$\eta'_{\eta\pi\pi}K^+$	$11.2^{+4.1}_{-3.4}$	30	5.1	$6.7^{+2.5}_{-2.1} \pm 0.8$
$\eta'_{\rho\gamma}K^+$	$19.6^{+6.6}_{-5.7}$	28	8.4	$7.0^{+2.4}_{-2.1} \pm 0.9$
$\eta'_{5\pi}K^+$	$2.3^{+2.2}_{-1.5}$	17	1.7	$4.2^{+4.0}_{-2.7} \pm 1.4$
$\eta'_{\eta\pi\pi}K^0$	$1.4^{+1.7}_{-1.0}$	23	1.4	$3.1^{+3.7}_{-2.1} \pm 0.6$
$\eta'_{\rho\gamma}K^0$	$5.7^{+3.7}_{-2.8}$	27	2.8	$6.2^{+4.0}_{-3.0} \pm 1.2$
$\eta'_{\eta\pi\pi}\pi^+$	$1.4^{+2.2}_{-1.4}$	30	5.2	<3.7
$\eta'_{\rho\gamma}\pi^+$	$4.0^{+4.6}_{-3.3}$	29	8.8	<4.5
$\eta'_{5\pi}\pi^+$	$0.5^{+1.9}_{-0.5}$	18	1.8	<10.7
$\eta'_{\eta\pi\pi}\pi^0$	$0.0^{+0.5}_{-0.0}$	25	4.3	<1.8
$\eta'_{\rho\gamma}\pi^0$	$0.0^{+2.0}_{-0.0}$	29	8.7	<2.2
$\eta'_{\eta\pi\pi}\eta'_{\eta\pi\pi}$	$0.0^{+0.5}_{-0.0}$	19	0.6	<15.2
$\eta'_{\eta\pi\pi}\eta'_{\rho\gamma}$	$0.0^{+0.8}_{-0.0}$	19	1.7	<6.4
$\eta'_{\eta\pi\pi}\eta_{\gamma\gamma}$	$0.0^{+0.5}_{-0.0}$	26	1.8	<4.6
$\eta'_{\eta\pi\pi}\eta_{3\pi}$	$0.0^{+0.5}_{-0.0}$	17	0.7	<12.5
$\eta'_{\rho\gamma}\eta_{\gamma\gamma}$	$5.6^{+4.6}_{-3.6}$	28	3.3	<13.0
$\eta'_{\rho\gamma}\eta_{3\pi}$	$0.0^{+0.6}_{-0.0}$	16	1.1	<9.3
$\eta'_{\eta\pi\pi}K^{*+}_{K^+\pi^0}$	$0.0^{+1.0}_{-0.0}$	13	0.7	<18
$\eta'_{\eta\pi\pi}K^{*+}_{K^0\pi^+}$	$0.0^{+1.6}_{-0.0}$	15	0.6	$<24.$
$\eta'_{\eta\pi\pi}K^{*0}$	$0.0^{+0.7}_{-0.0}$	22	2.5	<3.9
$\eta'_{\eta\pi\pi}\rho^+$	$0.0^{+0.7}_{-0.0}$	12	2.0	<5.7
$\eta'_{\eta\pi\pi}\rho^0$	$0.0^{+0.5}_{-0.0}$	22	3.8	<2.3
$\eta_{\gamma\gamma}K^+$	$1.3^{+3.5}_{-1.3}$	46	17.9	<1.5
$\eta_{3\pi}K^+$	$0.0^{+2.5}_{-0.0}$	28	6.3	<3.1
$\eta_{\gamma\gamma}K^0$	$1.8^{+2.4}_{-1.6}$	32	4.2	<4.7
$\eta_{3\pi}K^0$	$0.0^{+0.5}_{-0.0}$	14	1.1	<8.6
$\eta_{\gamma\gamma}\pi^+$	$0.2^{+5.0}_{-0.2}$	47	18.2	<1.7
$\eta_{3\pi}\pi^+$	$0.0^{+1.8}_{-0.0}$	29	6.6	<2.6
$\eta_{\gamma\gamma}\pi^0$	$0.0^{+0.9}_{-0.0}$	33	13.0	<0.9
$\eta_{3\pi}\pi^0$	$0.0^{+1.5}_{-0.0}$	23	5.5	<2.7
$\eta_{\gamma\gamma}\eta_{\gamma\gamma}$	$1.1^{+1.7}_{-1.1}$	34	5.2	<3.0
$\eta_{\gamma\gamma}\eta_{3\pi}$	$0.0^{+1.3}_{-0.0}$	24	4.3	<2.9
$\eta_{3\pi}\eta_{3\pi}$	$0.0^{+0.5}_{-0.0}$	16	0.8	<9.8
$\eta_{\gamma\gamma}K^{*+}_{K^+\pi^0}$	$0.7^{+3.6}_{-0.7}$	25	3.3	<8.8
$\eta_{3\pi}K^{*+}_{K^+\pi^0}$	$0.0^{+1.2}_{-0.0}$	15	1.2	<11.7
$\eta_{\gamma\gamma}K^{*+}_{K^0\pi^+}$	$0.0^{+1.2}_{-0.0}$	24	2.1	<5.7
$\eta_{3\pi}K^{*+}_{K^0\pi^+}$	$0.0^{+1.0}_{-0.0}$	14	0.8	<16.0
$\eta_{\gamma\gamma}K^{*0}$	$5.2^{+4.0}_{-3.0}$	32	8.4	<4.6
$\eta_{3\pi}K^{*0}$	$0.0^{+0.8}_{-0.0}$	20	3.1	<3.6
$\eta_{\gamma\gamma}\rho^+$	$1.2^{+4.1}_{-1.2}$	24	9.9	<3.3
$\eta_{3\pi}\rho^+$	$2.5^{+4.1}_{-2.5}$	14	3.3	<11.2
$\eta_{\gamma\gamma}\rho^0$	$0.2^{+4.0}_{-0.2}$	36	14.3	<1.9
$\eta_{3\pi}\rho^0$	$0.0^{+1.1}_{-0.0}$	22	5.1	<2.7

The PDFs $\mathcal{P}_S$ and $\mathcal{P}_B$ are constructed as products of functions of the observables $\mathbf{x}_i$. The dependences of $\mathcal{P}_S$ on masses and energies are Gaussian, double-Gaussian, or Breit-Wigner functions, whose means, widths, etc., appear as the parameters $\vec{\beta}$ in Eq. (1). The background PDF $\mathcal{P}_B$ contains signal-like peaking components in its resonance mass projections, to account for real resonances in the background, added to smooth components for combinatoric continuum. The smooth components are low-order polynomials, except that for M we use an empirical shape [13] that accounts for the phase space limit at $M = E_b$. The dependences of both $\mathcal{P}_S$ and $\mathcal{P}_B$ on $\mathcal{F}$, S_K, and S_π are bifurcated Gaussian functions. We obtain the parameters $\vec{\beta}$ of $\mathcal{P}_S$ from separate fits to the simulated signal, and $\vec{\gamma}$ of $\mathcal{P}_B$ from fits to the data in a sideband region of the $\Delta E - M$ plane.

Results for our 42 B decay chains [14] appear in Table I. The row label subscripts denote secondary decays, including $\eta' \to \eta\pi^+\pi^-$ with $\eta \to \gamma\gamma$ ($\eta\pi\pi$), $\eta' \to \eta\pi^+\pi^-$ with $\eta \to \pi^+\pi^-\pi^0$ (5π), and $\eta \to \pi^+\pi^-\pi^0$ (3π). The table gives each branching fraction quoted as central value with statistical followed by systematic error, or as 90% confidence level upper limit. We include systematic errors from uncertainties in the PDFs, i.e., in $\vec{\beta}$ and $\vec{\gamma}$, obtained from a Monte Carlo convolution of the likelihood function with Gaussian resolution functions for these parameters, including their most important correlations. This procedure changes the upper limit by less than 10% in most cases. We also include systematic errors for reconstruction efficiencies and selection requirements, and quote upper limits computed with efficiencies 1 standard deviation below nominal.

TABLE II. Combined branching fraction results, with expectations from theoretical models.

Decay mode	$\mathcal{B}(10^{-5})$	Theory $\mathcal{B}(10^{-5})$
$B^+ \to \eta' K^+$	$6.5^{+1.5}_{-1.4} \pm 0.9$	0.7–4.1 [9,15,17]
$B^0 \to \eta' K^0$	$4.7^{+2.7}_{-2.0} \pm 0.9$	0.9–3.3 [15,17]
$B^+ \to \eta' \pi^+$	<3.1	0.8–3.5 [9,15,17]
$B^0 \to \eta' \pi^0$	<1.1	0.4–1.4 [15,17]
$B^0 \to \eta' \eta'$	<4.7	0.07–3.0 [15,17]
$B^0 \to \eta' \eta$	<2.7	0.4–4.4 [15,17]
$B^+ \to \eta' K^{*+}$	<13.	0.003–0.9 [9,15,17]
$B^0 \to \eta' K^{*0}$	<3.9	0.005–0.3 [15,17]
$B^+ \to \eta' \rho^+$	<4.7	0.8–5.7 [9,15,17]
$B^0 \to \eta' \rho^0$	<2.3	0.2–1.2 [15,17]
$B \to \eta K^+$	<1.4	0.02–0.5 [9,15,17]
$B^0 \to \eta K^0$	<3.3	0.007–0.2 [15–17]
$B^+ \to \eta \pi^+$	<1.5	0.2–0.8 [9,15–17]
$B^0 \to \eta \pi^0$	<0.8	0.2–0.4 [15,17]
$B^0 \to \eta \eta$	<1.8	0.006–1.4 [15–17]
$B^+ \to \eta K^{*+}$	<3.0	0.02–1.3 [9,15,17]
$B^0 \to \eta K^{*0}$	<3.0	0.003–0.5 [15–17]
$B^+ \to \eta \rho^+$	<3.2	0.8–4.4 [9,15–17]
$B^0 \to \eta \rho^0$	<1.3	0.01–0.9 [15–17]

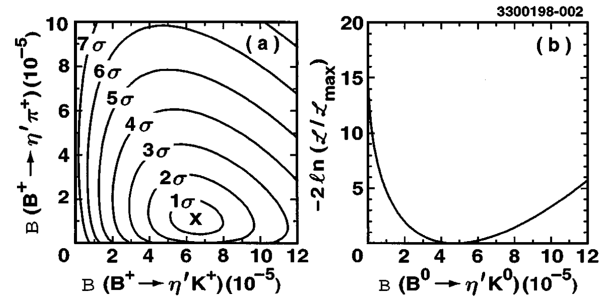

FIG. 2. (a) Likelihood function contours for $B^+ \to \eta' h^+$. (b) The function $-2 \ln \mathcal{L}/\mathcal{L}_{\max} = \chi^2 - \chi^2_{\min}$ for $B^0 \to \eta' K^0$.

Where we have measured a given B decay mode in more than one secondary decay channel we combine the samples by adding the $\chi^2 = -2 \ln \mathcal{L}$ functions of branching fraction and extracting a value with errors or limit from the combined distribution. The limit is the value of $\mathcal{B}$ below which 90% of the integral of $\mathcal{L}$ lies. The results are summarized in Table II, together with previously published theoretical calculations [9,15–17].

We have analyzed each of the decays also without use of the likelihood fit, employing more restrictive cuts in each of the variables to isolate the signals. The results are consistent with those quoted in the tables, but with larger errors (less restrictive limits) in most cases.

We find positive signals in both charge states of $B \to \eta' K$: $\mathcal{B}(B^+ \to \eta' K^+) = (6.5^{+1.5}_{-1.4} \pm 0.9) \times 10^{-5}$ and $\mathcal{B}(B^0 \to \eta' K^0) = (4.7^{+2.7}_{-2.0} \pm 0.9) \times 10^{-5}$. (The first error quoted is statistical, the second systematic.) The significance, defined as the number of standard deviations corresponding to the probability for a fluctuation from zero to our observed yield, is 7.5 for $B^+ \to \eta' K^+$ and 3.8 for $B^0 \to \eta' K^0$. The likelihood functions from the fits for $B \to \eta' h^+$ and $B^0 \to \eta' K^0$ are shown in Fig. 2. For these modes we also show in Fig. 3 the projections of event distributions onto the M axis. Clear peaks at the B meson mass are evident.

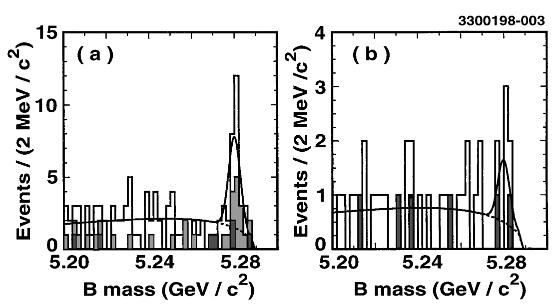

FIG. 3. Projections onto the variable M. Overlaid on each plot as smooth curves are the best fit functions (solid lines) and background components (dashed lines), calculated with the variables not shown restricted to the neighborhood of expected signal. The histograms show (a) $B^+ \to \eta' h^+$ with $\eta' \to \eta\pi\pi$ ($\eta \to 3\pi$, dark shaded areas), $\eta' \to \eta\pi\pi$ ($\eta \to \gamma\gamma$, light shaded areas), and $\eta' \to \rho\gamma$ (open areas); (b) $B^0 \to \eta' K^0$ with $\eta' \to \eta\pi\pi$ (shaded areas) and $\eta' \to \rho\gamma$ (open areas).

The observed branching fractions for $B \to \eta' K$, in combination with the upper limits for the other modes in Table II and with recent measurements of $B \to K\pi$ and $B \to \pi\pi$ [6], provide important constraints on the theoretical picture for these charmless hadronic decays. A large ratio of $B \to \eta' K$ to $B \to \eta K$, consistent with our measurements, was predicted [18] in terms of interference of the two penguin diagrams in Figs. 1(a) and 1(b), constructive for $B \to \eta' K$ and destructive for $B \to \eta K$. The effective Hamiltonian calculations [8] contain uncertainties in form factors [19,20], light quark masses [20], the QCD scale, and the effective number of colors. They generally employ spectator and factorization [21] approximations. The unexpectedly large branching fraction for $B \to \eta' K$ has led to a reevaluation of some of the older calculations. Recent suggestions include contributions from the QCD gluon anomaly or other flavor singlet processes [Fig. 1(d)] in constructive interference with the penguins [10,22–25]. Prospects are good for resolution of some of these issues as new data become available.

We thank A. Ali, T. DeGrand, P. Lepage, H. Lipkin, A. Kagan, and A. Soni for useful discussions. We gratefully acknowledge the effort of the CESR staff in providing us with excellent luminosity and running conditions. This work was supported by the National Science Foundation, the U.S. Department of Energy, the Heisenberg Foundation, Research Corporation, the Natural Sciences and Engineering Research Council of Canada, the A. P. Sloan Foundation, and the Swiss National Science Foundation.

*Permanent address: University of Texas, Austin, TX 78712.

†Permanent address: Lawrence Livermore National Laboratory, Livermore, CA 94551.

‡Permanent address: BINP, RU-630090 Novosibirsk, Russia.

§Permanent address: Yonsei University, Seoul 120-749, Korea.

‖Permanent address: Brookhaven National Laboratory, Upton, NY 11973.

[1] M. Kobayashi and T. Maskawa, Prog. Theor. Phys. **49**, 652 (1973).

[2] CLEO Collaboration, J. P. Alexander *et al.*, Phys. Rev. Lett. **77**, 5000 (1996).

[3] CLEO Collaboration, R. Ammar *et al.*, Phys. Rev. Lett. **71**, 674 (1993).

[4] CLEO Collaboration, M. Battle *et al.*, Phys. Rev. Lett. **71**, 3922 (1993).

[5] CLEO Collaboration, D. M. Asner *et al.*, Phys. Rev. D **53**, 1039 (1996).

[6] CLEO Collaboration, R. Godang *et al.*, Report No. CLNS 97/1522 (to be published).

[7] See, for instance, Michael Gronau and Jonathan L. Rosner, Phys. Rev. D **53**, 2516 (1996); A. S. Dighe, Phys. Rev. D **54**, 2067 (1996); M. Gronau and J. L. Rosner, Phys. Rev. Lett. **76**, 1200 (1996).

[8] A. Ali and C. Greub, Report No. DESY 97-126, 1997; N. G. Deshpande, B. Dutta, and S. Oh, Report No. OITS-641, 1997, and references therein.

[9] G. Kramer, W. F. Palmer, and H. Simma, Z. Phys. C **66**, 429 (1995).

[10] A. S. Dighe, M. Gronau, and J. L. Rosner, Phys. Rev. Lett. **79**, 4333 (1997); D. London and A. Soni, Phys. Lett. B **407**, 61 (1997).

[11] CLEO Collaboration, Y. Kubota *et al.*, Nucl. Instrum. Methods Phys. Res., Sect. A **320**, 66 (1992).

[12] GEANT 3.15: R. Brun *et al.*, Report No. CERN DD/EE/84-1, 1984.

[13] With $x \equiv M/E_b$ and ξ a parameter to be fit, $f(x) \propto x\sqrt{1 - x^2}\exp[-\xi(1 - x^2)]$ [see H. Albrecht *et al.*, Phys. Lett. B **241**, 278 (1990); **254**, 288 (1991)].

[14] Inclusion of the charge conjugate states is implied in the row labels and throughout this paper.

[15] L.-L. Chau *et al.*, Phys. Rev. D **43**, 2176 (1991). A private communication from H-Y. Cheng indicates that many of the η' and η branching fraction predictions in this paper were too large. The revised prediction for $\mathcal{B}(B^+ \to \eta' K^+)$ is 1.9×10^{-5}. See also Ref. [24].

[16] A. Deandrea *et al.*, Phys. Lett. B **318**, 549 (1993); **320**, 170 (1994).

[17] D. Du and L. Guo, Z. Phys. C **75**, 9 (1997).

[18] H. J. Lipkin, Phys. Lett. B **254**, 247 (1991); this effect is incorporated in the predictions cited in Table II.

[19] A. Datta, X-G. He, and S. Pakvasa, Report No. UH-511-864-97, 1997.

[20] A. Kagan and A. Petrov, Report No. UCHEP-27, 1997.

[21] M. Bauer, B. Stech, and M. Wirbel, Z. Phys. C **43**, 103 (1987).

[22] David Atwood and Amarjit Soni, Phys. Lett. B **405**, 150 (1997).

[23] M. R. Ahmady, E. Kou, and A. Sugamoto, Report No. RIKEN-AF-NP-274, 1997; D. Du, C. S. Kim, and Y. Yang, Report No. BIHEP-TH/97-15, 1997.

[24] H-Y. Cheng and B. Tseng, Report No. IP-ASTP-03-97, 1997.

[25] Igor Halperin and Ariel Zhitnitsky, Phys. Rev. D **56**, 7247 (1997).